Volume 1 | Number 1 | Jan 2013 | Pages 1–100

Journal of
Materials Chemistry A

Materials for energy and sustainability
www.rsc.org/materialsA

Li⁺

ROYAL SOCIETY
OF CHEMISTRY

ROYAL SOCIETY
OF **CHEMISTRY**

www.rsc.org/materialsA

Journal of Material Chemistry A

ARTICLE

Enhanced thermoelectric performance of PEDOT with different counter-ions optimized by chemical reduction

M. Culebras, C. M. Gómez and A. Cantarero

This work reports on the synthesis by electro-polymerization and the thermoelectric properties of the intrinsically conducting polymer poly(3,4-ethylenedioxythiophene) (PEDOT) doped with several counter-ions: ClO_4, PF_6 and bis(trifluoromethylsulfonyl)imide (BTFMSI). We show that, depending on the counter-ion size, the thermoelectric efficiency of PEDOT can be increased up to two orders of magnitude. A further chemical reduction with hydrazine optimizes the power factor (PF). By changing the counter-ions, we were able to increase the electrical conductivity (σ) of PEDOT by a factor of three, while the Seebeck coefficient remains at the same order of magnitude in the three polymers. The best thermoelectric efficiency has been observed in PEDOT:BTFMSI. From the measurement of the Seebeck coefficient and σ, a PF of 147 $\mu Wm^{-1}K^{-2}$ has been deduced, while the measured thermal conductivity is κ=0.19 $Wm^{-1}K^{-1}$, resulting in a $ZT \sim 0.22$ at room temperature, one of the highest values supplied in the literature for polymers. The increase in σ with the change of the counter-ion is mainly due to the stretching of the polymer chains. In this work, we provide a chemical route to further improve ZT in polymers and give a method of synthesis based on the electro-polymerization on gold. After removing the gold layer, a very thin semiconducting polymer film can be isolated.

Introduction

Since the discovery of the thermoelectric phenomena by Seebeck, Peltier and Thomson in the earlier 1800s, several semiconductors and semiconductor alloys have been extensively investigated for the fabrication of thermoelectric modules. A thermoelectric generator (TEG) is a device able to convert heat into electricity; in other words, a TEG can harvest electricity directly from waste heat or from natural resources. The efficiency of a thermoelectric (TE) material is proportional to the dimensionless figure of merit:

$$ZT = \frac{S^2 \sigma T}{\kappa} \quad (1)$$

where S is the Seebeck coefficient and σ and κ are the electrical and thermal conductivities, respectively. The thermal conductivity has two contributions, since both the electrons and the lattice transport heat. In metals, the electronic contribution dominates, while in semiconductors the contribution of the lattice dominates. Since ZT is proportional to the absolute temperature T, the figure of merit cannot be constant as a function of T. There is a maximum value at a certain temperature, depending on the material. In this way, a good thermoelectric material at high temperatures can have a very low ZT at low temperatures and vice-versa.

During the 1950's, different inorganic semiconductor compounds, such as Bi_2Te_3, or ternary alloys incorporating Pb, were found to have a value of ZT of 0.6-0.7 at room and higher temperatures.[1] This was the highest efficiency attained until 1993. At that time, Hicks and Dresselhaus showed a path to increase the thermoelectric efficiency of a semiconductor: the reduction of the dimensionality.[2] Following their ideas, semiconductor superlattices such as Bi_2Te_3/Sb_2Te_3,[3] semiconductors alloys like PbSeTe [4] or, more recently, SiGe [5] have been shown to have ZT values around 2. In the last years, the reduction of the dimensionality in Si by growing it in the form of nanowires has proven to be an effective way to decrease the phonon thermal conductivity. Si nanowires with rough surfaces favor a further decrease of the thermal conductivity by the appearance of back-scattering phonon processes. Since S and σ are somehow related in semiconductors, [6, 7] the engineering to decrease κ is the most

effective tool to increase *ZT*. [8] In spite of the efforts to increase *ZT* in inorganic materials, it seems that the limit in the case of superlattices is of the order of 2, and there are no advances in the fabrication of TEG based on nanowires in the last years. On the other hand, when we compare semiconductor-based TEG with that based on organic materials, we can find several drawbacks in inorganic semiconductors. 1) The first one is the high cost of production of semiconductors with good TE properties. As a result, a tiny amount of n- and p-doped Bi_2Te_3, is used in commercial TEGs; 2) The second problem is the high toxicity of some of the compounds, that containing Pb for instance. Finally, 3) the scarcity of materials. For this reason, many researches have driven their efforts in the search of new and clean ("green") efficient thermoelectric materials during the last years.

Intrinsically conducting polymers (ICPs) such as polyaniline [9], polythiophene, [10] poly(3,4-ethylenedioxythiophene): poly(styrenesulfonate) [11] and polycarbazoles [12] show a great potential as materials for thermoelectric applications. Additionally to the arguments supplied in the previous paragraph, ICPs present some advantages compared with inorganic compounds in the field of thermoelectricity. They show an easier chemical modification, the abundance and low cost of raw materials, they have a low thermal conductivity and show, in general, good mechanical properties. However, up to now, their efficiency was much lower than that of semiconductor-based thermoelectric devices. In particular, PEDOT-based polymers represent a great potential for thermoelectric applications. The most studied PEDOT derivative in the literature is PEDOT:PSS due to their inherent properties such as water solubility, low cost and commercial availability. In general, low *ZT* values have been reported in the past for this material. For example, $ZT\sim10^{-4}$ for PEDOT:PSS doped with dimethyl sulfoxide (DMSO) and $ZT\sim10^{-3}$ with DMSO. [13, 14, 15, 16] However, when the counter-ion is tosilate (Tos), the thermoelectric performance of PEDOT increases up to $ZT\sim10^{-2}$ for a high oxidation level. [17] Many researchers tried to increase the thermoelectric efficiency of PEDOT:PSS with the addition of nanofillers such as carbon nanotubes (CNT), [18] PbTe [19] or expanded graphite. [20] Other considerations to maximize *ZT* is to change the doping level in the ICPs, in order to obtain a better power factor *PF* ($PF = S^2 \cdot \sigma$) to optimize *ZT*. Good results have been obtained for PEDOT:Tos reduced by chemical and electrochemical methods, *ZT*= 0.25, in the case of chemical reduction [17, 21] .

In this work, we have synthesize, via electrochemical deposition, different PEDOT derivatives: PEDOT:ClO₄, PEDOT:PF₆ and PEDOT:bis(trifluoromethylsulfonyl)imide (PEDOT:BTFMSI), which are used for the first time for thermoelectric applications. By changing the size of the counter-ion, we expect to modify the conductive properties of the PEDOT-based polymers. With the electrochemical process presented in this work, we are able to produce homogeneous thin films with very high electrical conductivity. The electro-polymerization is a cheap method to synthesize conducting polymers as polypyrrole, polyaniline and PEDOT:ClO₄. This method present several advantages (fast polymerization, lack of purification steps and scalability), which makes it very interesting for industrial applications.

Results and discussion

For the morphological characterization of the film surface, we have used a scanning electron microscope. Figure 1 shows the scanned (SEM) images of the three films surfaces under study. All the films appear to be homogeneous and compact with different roughness degree. Figures 1A and 1B (PEDOT:ClO₄) show a very rough surface, with well distinguished globules, homogeneously distributed all over the surface. This film resembles compact with ordered arrangements of cauliflowers-shaped granules, typical of electro-synthesized films. On the other hand, the Figures 1C, 1D, 1E and 1F (PEDOT:PF₆ and PEDOT:BTFMSI films) depict a smoother surface of nearly interconnected polymer chains and voids in between. [13] A smoother, more homogeneous and compact polymer film will clearly improve the electrical conductivity and the electron transfer capability between chains due to a more stretched polymer structure. The reduction treatment does not alter the morphology of the films as shown in Figures 1B, 1D and 1F.

A Raman study (Figure 2) has also been performed in the three polymers synthetized in this work in order to analyze the effect of the reduction on the vibrational modes of PEDOT also. The spectra depicts different vibrational modes, at 440, 576 and 990 cm⁻¹, the modes related to the oxyethylene ring deformation; the peak at 691 cm⁻¹ corresponds to the symmetric C-S-C deformation; the C-O-C deformation corresponds to the mode appearing at 1100 cm⁻¹; the C_α-C_α (inter-ring) stretching mode is located at 1260 cm⁻¹; the peak at 1361 cm⁻¹ is related to the C_β-C_β stretching; the symmetric stretching mode C_α=C_β(-O) appears at 1430 cm⁻¹, and the asymmetric stretching of C = C split, as it is well know, into two Raman peaks at 1508 cm⁻¹ and 1568 cm⁻¹, respectively. The frequencies of all the modes found in the Raman spectra are given in Table 1. These spectra are a test showing that PEDOT has been obtained after the electrochemical synthesis [22].

The normalized signals show a clear increase in the intensity of the peaks centred at 1300-1500 cm⁻¹, respect to the background signal, with the reduction time. This effect is due to the fact that the neutral segments of PEDOT are more active than the doped segments at the excitation line of 514.53 nm (green). Consequently, when the sample is subjected to the reduction treatment with hydrazine, the number of neutral segments increases, resulting in an increase of Raman signal. These results are in agreement with the Raman studies of doping in PEDOT previously published by S. Garreau et al. [22, 23]

The UV-Vis-NIR absorption as a function of the reduction time is presented in Figure 3. The spectra obtained for highly reduced PEDOT:ClO₄, PEDOT:PF₆ and PEDOT:BTFMSI (25 s

of reduction time) show a broad absorption band centered around 600 nm, that correspond to the π-π* transition (valence to conduction transition in a semiconductor), associated with the neutral segments in the PEDOT chains [22]. The other band observed in the UV-Vis-NIR spectra appears around 900 nm. This band is related to the doping process of ICPs, actually due to bipolaron states [24]. The UV-Vis-NIR results indicate a clear influence of the reduction time with the doping level in the three polymers synthetized. In all cases the band centered around 600 nm increases with reduction due to the de-doping process, since they produce an increase of the neutral polymer segments. Also, the high NIR absorption in highly doped samples decreases with the reduction process, and it has been assigned to the decrease of bipolaron states [25].

Figure 4 depicts the values of the electrical conductivity σ, the Seebeck coefficient S, and the power factor *PF*, of PEDOT:ClO$_4$, PEDOT:PF$_6$ and PEDOT:BTFMSI films as a function of the chemical reduction time. Note that increasing the reduction time up to 2 min gives the same values already obtained with 20 s. As shown in Figure 4, the electrical conductivity decreases with the reduction time until reaching a plateau due to the saturation of the doping level. After chemical reduction, the electrical conductivity changes from 753 to 230 S/cm for PEDOT:ClO$_4$, from 1000 to 312 S/cm in the case of PEDOT:PF$_6$ and from 2074 to 708 S/cm for PEDOT:BTFMSI. The opposite behavior has been observed in the variation of the Seebeck coefficient with the reduction time

Although the Seebeck coefficient is small, it increases with reduction time: from 9 to 35 µV/K for PEDOT:ClO$_4$, from 11 to 34 µV/K in the case of PEDOT:PF$_6$ and from 14 to 42 µV/K for PEDOT:BTFMSI after 25 s of reduction time. These values are higher than those obtained for the PEDOT: PSS (S~15 µV/K) [13, 14, 15, 16] but lower than that of PEDOT:Tos (40-700 µV/K) [17]. In Figure 4, we also plot the power factor in order to show the optimum reduction time providing the highest thermoelectric efficiency. Figure 4 indicates that the optimum reduction time for de three polymers studied is around 11 s with 41 µW/mK^2 for PEDOT:ClO$_4$; 11 s with 60 µW/mK^2 for PEDOT:PF$_6$ and 5 s with 147 µW/mK^2 for PEDOT:BTFMSI. As reported in the literature, polymeric materials with high doping level show a high electrical conductivity and a low Seebeck coefficient [17,21]. When the doping level decreases, the Seebeck effect increases while the electrical conductivity decreases. The best compromise is given by the best power factor (*PF*=S^{2}σ).   PEDOT:ClO$_4$,   PEDOT:PF$_6$ and PEDOT:BTFMSI are initially oxidized (highly doped). By reducing them with hydrazine, the doping level decreases up to reach the optimum *PF*. The reduction times, in our case, are of the order of a few seconds since we are dealing with undiluted hydrazine. These results are very exciting when compared with other ICPs. [26, 27] The electrical conductivity obtained for PEDOT:ClO$_4$ and PEDOT:PF$_6$ is very similar when compared with PEDOT:PSS doped with DMSO[28, 29] (800-1000 S/cm),

but in the case of PEDOT: BTFMSI is relatively high and of the same order that PEDOT:Tos (2120 S/cm) [21].

The polymer conformation may play an important role in its physical properties, in particular in the conductivity. The electron-hole interaction leads to strongly bonded excitons (Frenkel excitons), which greatly affects the transport properties in conducting polymers. In the case of PEDOT, the electronic transport is traditionally explained by the charge-energy-limited-tunneling model, proposed originally for highly disordered ICPs. [30, 13] Looking at Figure 1 and the evolution of the electrical conductivity in the three polymers, clearly a great change from the typical coil conformation to a linear or expanded-coil conformation takes place in the presence of different counter-ions or dopants. The evolution of the chain conformation with the increase of the counter-ion increases the compactness of the films, producing an increase of the electrical conductivity. Thus, the increasing order in the electrical conductivity (PEDOT:BTFMSI > PEDOT:PF$_6$ > PEDOT:ClO$_4$) is strongly related with the conformation of the PEDOT chains caused by the increase in the size of the three counter-ions used as shown schematically in Figure 5**.**

In general, amorphous polymers adopt a coil form. Thus, small anions such as perchlorate$_s$ may lie smoothly neutralizing the positive charges of the chain, without modifying the coil structure. The increase in counter-ion size produces an extension of the polymer chain due to electrostatic interaction. An extended chain is more favorable for the neutralization of the positive charges of PEDOT by the BTFMSI anions, leading to an increase of the electrical conductivity. The fact that the extended chains are more conductive than coil chains is well known in the literature. For example, PEDOT:PSS doped with DMSO or EG and polyaniline doped with m-cresol [13, 31].

The thermal conductivity of our samples have been measured using a MDSC system according to the ASTM E1952-11 standard. The values obtained at 25 ºC were 0.35±0.02 W m^{-1}K^{-1} for PEDOT:ClO$_4$, 0.22±0.02 W m^{-1}K^{-1} for PEDOT:PF$_6$ and 0.19±0.02 Wm^{-1}K^{-1} for PEDOT:BTFMSI. We have checked that the thermal conductivity does not change with the reduction level. These values are very similar to that calculated for PEDOT:Tos (0.37 W m^{-1}K^{-1}) and PEDOT:PSS (0.20 W m^{-1}K^{-1}). [17, 13] The figure of merit, calculated from Equation (1) for all reductions times, is shown in Figure 6. The best value have been obtained for PEDOT:BTFMSI, *ZT*~0.22. This value is one of the highest reported for polymers in the literature, approaching to the record value obtained for a polymer [29] (ZT= 0.4).

The importance of these high *ZT* values is the fact that they have been obtained within the polymer matrix, without the need of additional fillers. For this reason, it is interesting to compare our results with the most relevant data published on the thermoelectric performance in polymer composites. For example: in PANI/Bi nanocomposites *ZT*~0.4-1.3×10^{-3} [32], in PANI/SWCNTs [33], *ZT*~0.4-1.3×10^{-3}, in poly(3-

hexylthiophene)/Bi$_2$Te$_3$ nanocomposites [34] $ZT \sim 1.7 \times 10^{-2}$, in PEDOT:PSS/SWCNTs[18, 35], $ZT \sim 2 \times 10^{-2}$ or PEDOT:PSS/CNT-stabilizers (PF 500 μW m^{-1} K^{-2}) and, finally, in PEDOT:PSS/Te films [36] $ZT \sim 0.1$. In addition, the suitable experimental process for manufacturing nanocomposites without purification stages indicates that PEDOT:ClO$_4$, PEDOT:PF$_6$ and PEDOT:BTFMSI could be good candidates as polymer matrices in the production of high thermoelectric efficiency nanocomposites with high *ZT* values.

Experimental

Materials and methods.

The reactants used in this study, 3,4-Ethylenedioxythiophene, Lithium perchlorate (LiClO$_4$), 1-Butyl-3-methylimidazolium hexafluorophosphate, 1-Ethyl-3-methylimidazolium bis(trifluoromethylsulfonyl)imide and acetonitrile, were purchased to Sigma Aldrich Co. Figure 7 shows the structure of these molecules.

The films of PEDOT:ClO$_4$, PEDOT:PF$_6$ and PEDOT:BTFMSI were synthesized through electrochemical polymerization on a gold surface (20 nm) previously deposited on a glass substrate (2 × 4 cm^2) by metal evaporation in a Univex 300 Evaporation system [37,38]. The gold layer was, at the same time, the working electrode. The PEDOT:ClO$_4$, PEDOT:PF$_6$ and PEDOT: BTFMSI were polymerized starting from a 0.01 M solution of EDOT and LiClO$_4$ 0.1 M, 1-Butyl-3-methylimidazolium hexafluorophosphate 0.01 M, 1-Ethyl-3-methylimidazolium bis(trifluoromethylsulfonyl)imide 0.01 M, respectively, in 100 ml of acetonitrile at -3 mA versus an Ag/AgCl reference electrode during 2 minutes. Under these experimental conditions, the thickness was 110-120 nm. A Pt grid was used as counter electrode and a Keithley 2400 power supply was employed. The gold layer was removed with an acid solution (HNO$_3$:HCl ratio 1:3) after the polymer films were obtained to allow transport measurements on the polymer films. The PEDOT derivatives thin films were washed several times with water and finally with ethanol (with this treatment, the gold layer was removed keeping the polymer integrity and their properties, see supporting information).

The resulting films of PEDOT:ClO$_4$, PEDOT:PF$_6$ and PEDOT:BTFMSI were reduced by contact with hydrazine (N$_2$H$_4$) vapor during several seconds. In order to guarantee the reproducibility, the procedure was to optimize the *PF* keeping constant the hydrazine steam flow through the film surface, i.e. the film surface was in close contact with the hydrazine vapor. Figure 8 depicts a scheme of the polymer surface formation,

Characterization

In order to perform the electrical characterization, six gold contacts were coated on the polymer film surface by thermal evaporation; they were also used for the thermoelectric measurements. The electrical conductivity was obtained with the van der Pauw method. This method can be utilized to determine the conductivity of thin films whenever the distance between contacts is much larger than the sample thickness; additionally since the resistance measurements were carried out by using four contacts, it is independent of contact resistance. Actually, the electrical conductivity has been obtained by solving numerically the van der Pauw equation:

$$e^{-\pi \cdot d \cdot R_1 \cdot \sigma} + e^{-\pi \cdot d \cdot R_2 \cdot \sigma} = 1 \qquad (2)$$

where σ is the conductivity, *d* the sample thickness, and R_1 and R_2 the resistance values. To calculate R_1 and R_2, four contacts, labeled as *A*, *B*, *C* and *D*, were used. $R_1 = V_{BD} / I_{AC}$ and $R_2 = V_{AB} / I_{CD}$, were *V* and *I* are the voltage and intensity across the sample. The thickness of the films was measured with a profilometer.

The Seebeck coefficient is determined as the ratio between the electrical potential, ΔV, and the temperature difference, ΔT, that is:

$$S = \frac{\Delta V}{\Delta T} \qquad (3)$$

The SEM analysis was carried on a Hitachi 4800 S microscope at an acceleration voltage of 20 kV and at a working distance of 14 mm for gold-coated surfaces.

The PEDOT was characterized by Raman spectroscopy. The Raman spectroscopy analysis was performed in a Jobin Yvon T64000 spectrometer coupled to an Olympus microscope. The excitation source was a Kr-Ar laser (Spectrum 70, from Coherent). The excitation wavelength was 514.53 nm. The Raman signal was measured with an open-electrode CCD detector in the 200 cm^{-1} - 1800 cm^{-1} range with and the acquisition time was 100 seconds.

The absorbance measurements were carried out in a Shimadzun UV-2501PC UV-Vis spectrophotometer from 1100 to 300 nm.

The thermal conductivity was determined with the aid of modulated differential scanning calorimetry (MDSC) according to the ASTM E1952-11 standard test method. This method is valid to measure thermal conductivities of polymeric materials with values within the range 0.1-1 Wm^{-1}K^{-1}. The MDSC measurements were performed in a DSC Q-20 TA instruments calibrated with indium and sapphire. All MDSC measurements were carried out at 300 K in modulated conditions with a period of 80 s and ±1 K of temperature amplitude.

Conclusions

Intrinsically conducting polymers with high electrical conductivity have been prepared using a very simple technique: electro-polymerization. Depending on the type of counter-ions used in the polymer synthesis, the surface of the samples show different morphologies, as observed in the SEM images. The electrical conductivity decreases with the reduction time, while the Seebeck coefficient increases. The maximum ZT has been obtained for 11 seconds of reduction in the case of PEDOT:ClO$_4$ and PEDOT:PF$_6$ and 5 seconds for PEDOT:BTFMSI, these reduction times gives Seebeck and electrical conductivity optimum values for a maximum thermoelectric efficiency, corresponding to the best PF. The maximum ZT obtained in this work is of the same order of some inorganic materials. This fact indicates that more effort must be oriented to the development of organic materials since clearly they can compete with inorganic materials in thermoelectric applications.

Acknowledgements

Notes and references

Materials Science Institute, University of Valencia PO Box 22085, 46071 Valencia, Spain.

Electronic Supplementary Information (ESI) available: [details of any supplementary information available should be included here]. See DOI: 10.1039/b000000x/

1   H. J. Goldsmid, *J. Electronics.* 1955, **1**, 218.

2   L. D. Hicks and M. S. Dresselhaus, *Phys. Rev.* B, 1993, **47**, 12727.

3   R. Venkatasubramanian, E. Slivola, T. Colpitts, B. O'Quinn, *Nature*, 2001, **413**, 597.

4   T. C. Harman, P. J. Taylor, M. P. Walsh, B. E. LaForge, *Science*, 2002, **297**, 2229.

5   X. W. Wang, H. Lee, Y. C. Lan, G. H. Zhu, G. Joshi, D. Z. Wang, J. Yang, A. J. Muto, M. Y. Tang, J. Klatsky, S. Song, M. S. Dresselhaus, G. Chen, Z. F. Ren, *Appl. Phys. Lett*, 2008 , **93** , 193121.

6   A. Cantarero and F. X. Àlvarez, Thermoelectric effects: semiclassical and quantum approaches to the Boltzmann transport equation, in Nanoscale Thermoelectrics, p. 1-39, Springer 2014.

7   R. D'Agosta, Phys. Chem. Chem. Phys. 2013, **15**, 1758.

8   A. I. Boukai, Y. Bunimovich, J. Tahir-Kheli, J. K. Yu, W. A. Goddard, J. R. Heath, *Nature*, 2008, **451**, 168.

9   N. Toshima, *Macromol Symp,* 2002, **186**, 81.

10   B.Y. Lu, C.C. Liu, S. Lu, J. K. Xu, F. X. Jiang, Y.Z. Li, Z. Zhang, *Chin Phys Lett,* 2010, **27**, 057201.

11   B. Zhang, J. Sun, H. E. Katz, F. Fang, R. L.Opila, *ACS Appl. Mater. Interfaces,* 2010, **2**, 3170.

12   N. Dubey, M. Leclerc, *J. Polym. Sci. Pt. B-Polym. Phys,* 2011, **49**, 467.

13   F. X. Jiang, J. K. Xu, B.Y. Lu, Y. Xie, R.J. Huang, L.F. Li, *Chin Phys Lett,* 2008, **25**, 2202.

14   M. Scholdt, H. Do, J.Lang, A. Gall, A. Colsmann,U. Lemmer, J. D. Koenig, M.Winkler, H. Boettner, *J. Electron. Mater,* 2010, **39**, 1589.

15   K. C. Chang, M. Y. Jeng, C. C. Yang, Y. W Chou, S. K. Wu, M. A. Thomas, Y. C. Peng, *J. Electron. Mater,* 2009, **38**, 1182.

16   C. Liu, B. Lu, J. Yan, J. Xu, R. Yue, Z. Zhu, S. Zhou, X. Hu, Z. Zhang, P. Chen, *Synth. Met,* 2010, **160**, 2481.

17   O. Bubnova, Z.U. Khan, A. Malti, S. Braun, M. Fahlman, M. Berggren, X. Crispin. *Nat. Mater*, **2012**, 10, 429.

18   D. Kim, Y. Kim, K. Choi, J. C. Grunlan, C. H. Yu, *ACS Nano,*2010, **4**, 513.

19   Y. Wang, K. Cai, X. Yao, *ACS Appl. Mater. Interfaces,* 2011, **3**, 1163.

20   M. Culebras, C. M. Gómez, A. Cantarero, *J Mater Sci,* 2013, **48**, 2855.

21   T. Park, C. Park, B. Kim, H. Shin, E. Kim, *Energy Environ. Sci,* 2013, **6**, 788.

22   S. Garreau, G. Louarn, J. P. Buisson, G. Froyer, S. Lefrant, *Macromolecules*, 1999, **32**, 6807.

23   S. Garreau, J. L. Duvail, G. Louarn, *Synth. Met*, 2002, **125**, 325.

24   X. Chen. O. Inganaes, *J. Phys Chem,* 1996, **100**, 15202.

25   A. O. Patil, A. J. Heeger, F. Wudl, *Chem. Rev.* 1988, **88**, 183.

26   F. Yakuphanoglu, B.F. Senkal and A. Sarac, *J. Electron. Mat*, 2008**, 37**, 930.

27   R. Yue, S. Chen, B. Lu, C. Liu and J. Xu, *J. So. Stat Electrochem*, 2011, **15**, 539.

28   J. Gasiorowski , R. Menon, K. Hingerl, M. Dachev, N. S. Sariciftci. *Thin solid films,* 2013, **536**, 211.

29   G. H. Kim, L. Shao, K. Zhang and K. P. Pipe, *Nat. Mater*, 2013, **12**, 719.

30   A. N. Aleshin, S. R. Williams, A. J. Heeger, *Synth. Met*, 1998, **94**, 173.

31   N. Kuramoto, *Preprints of Symposia - American Chemical Society, Division of Fuel Chemistry* ,(2012), **57**, 84.

32   S. R. Hostler, ITHERM, Thermal and Thermomechanical Phenomena in Electronics Systems, San Diego CA, May-June, 2006.

33   Q. Yao, L. Chen, W. Zhang, S. Liufu, K. Chen, *ACS Nano,*2010, **4**, 2445.

34   Y. Du, MIME, Preparation and thermoelectric properties of Bi$_2$Te$_3$/Polythiophene nanocomposite materials, Melbourne, January **2011**.

35   G.P. Moriarty, K. Briggs, B. Stevens, C. Yu, J.C. Grunlan, *Energy Technology,* 2013, **1**, 265.

36   K. C. See, J. P. Feser, C. E. Chen, A. Majumdar, J. J. Urban, R. A. Segalman, *Nano. Lett*, 2010, **10**, 4664.

37   J. Joo, K. T. Park, B. H. Kim, M. S. Kim, S. Y. Lee, C. K. Jeong, J. K. Lee, D. H. Park, W. K. Yi, S. H. Lee, K. S. Ry, *Synth. Met*. 2003, **135-136**, 7.

38   Y. Cao, A. E. Kovalev, R. Xiao, J. Kim, T. S. Mayer, T.E. Mallouk, *Nano. Lett*, 2008, **8**, 4653.
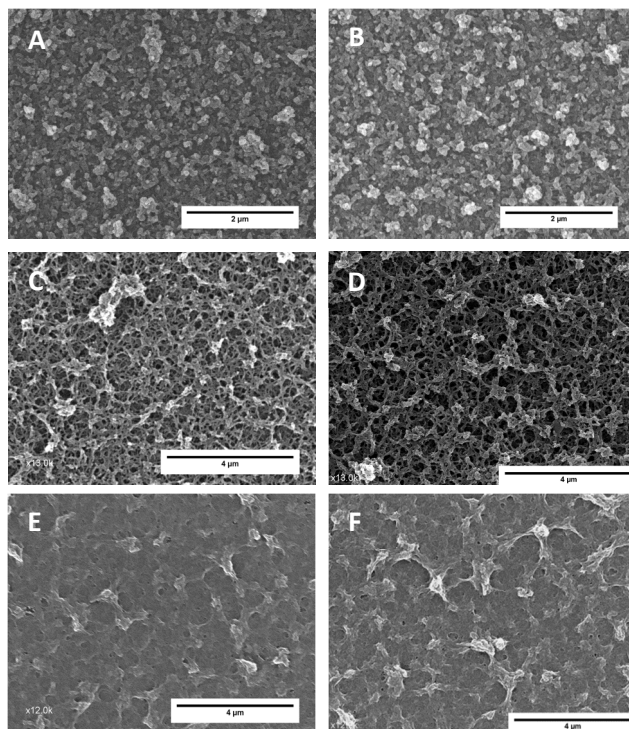
Figure 1. SEM images of A, native PEDOT:ClO$_4$, B, PEDOT:ClO$_4$ afther 20s of reduction treactament, C, native PEDOT:PF$_6$, D, PEDOT:PF$_6$ afther 20s of reduction treactament, E, native PEDOT:BTFMSI and D, PEDOT:BTFMSI afther 20s of reduction treactament showing the different morphologies.

Table 1. Typical vibrational modes of PEDOT.

Raman shift (cm^{-1})	Assignation
440	Oxyethylene ring def
576	Oxyethylene ring def
691	sym C-S-C def
990	Oxyethylene ring def
1100	C-O-C def
1260	C_α-C_α (inter-ring) str
1361	C_β-C_β-str
1430	sym C_α=C_β(-O) str
1508-1568	asym C=C str
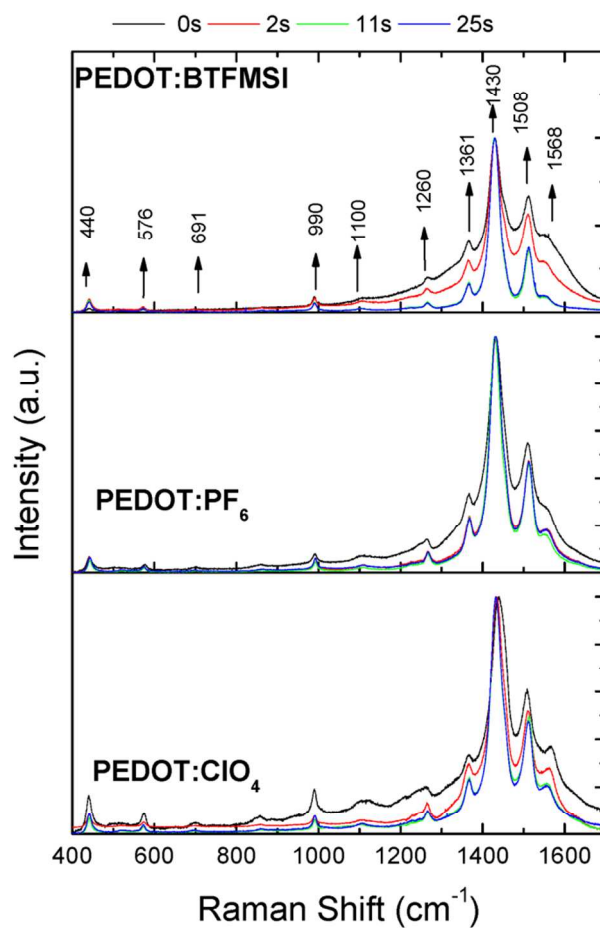
Figure 2. Raman spectra of PEDOT:ClO$_4$, PEDOT:PF$_6$ and PEDOT:BTFMSI at several reduction times.
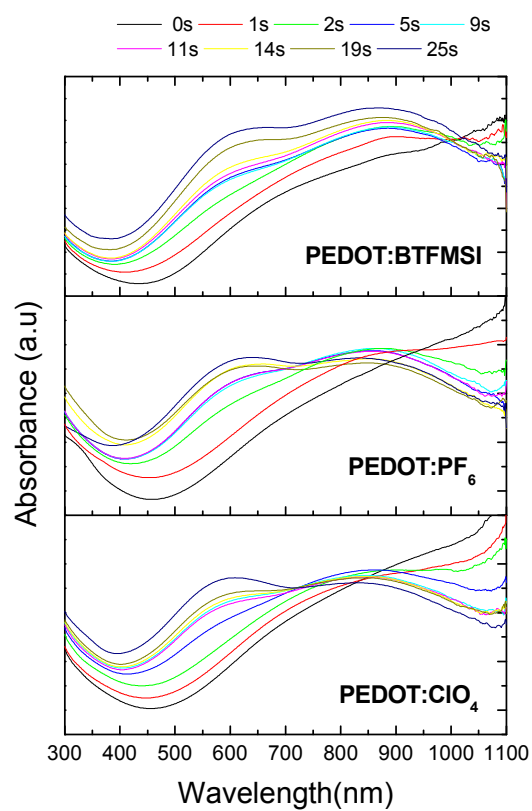
Figure 3. UV-Vis-NIRs spectra of PEDOT:ClO$_4$, PEDOT:PF$_6$ and PEDOT:BTFMSI at several reduction times.
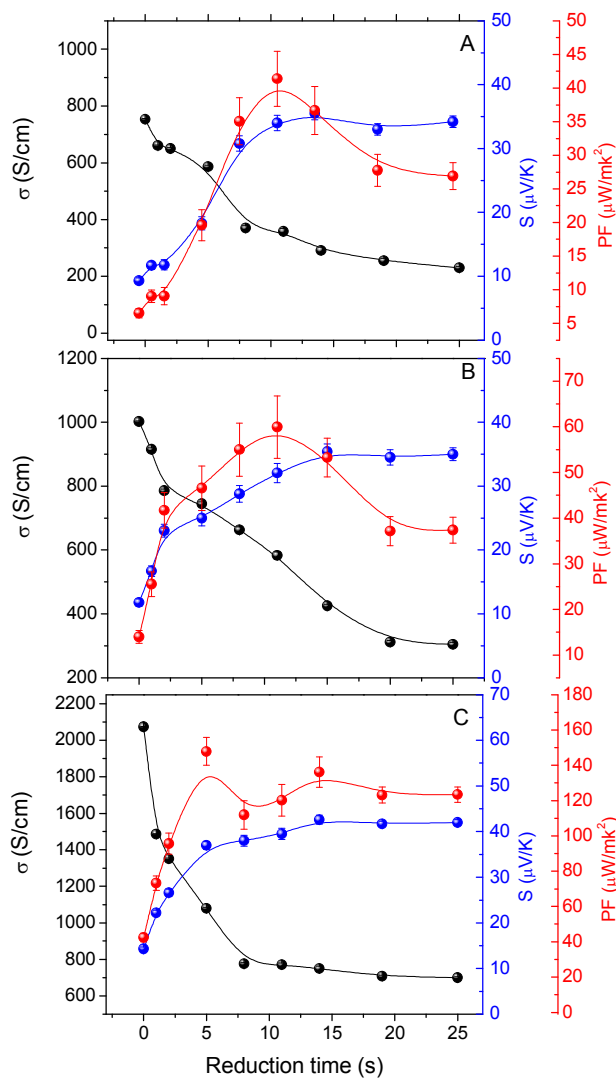
Figure 4. Electrical conductivity σ, Seebeck coefficient S, and power factor *PF*, of: (A) PEDOT:ClO$_4$, (B) PEDOT:PF$_6$ and (C) PEDOT:BTFMSI, as a function of chemical reduction time.
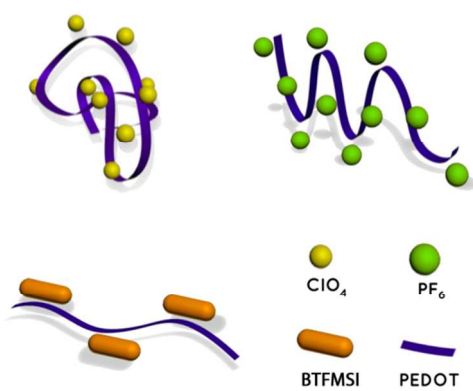
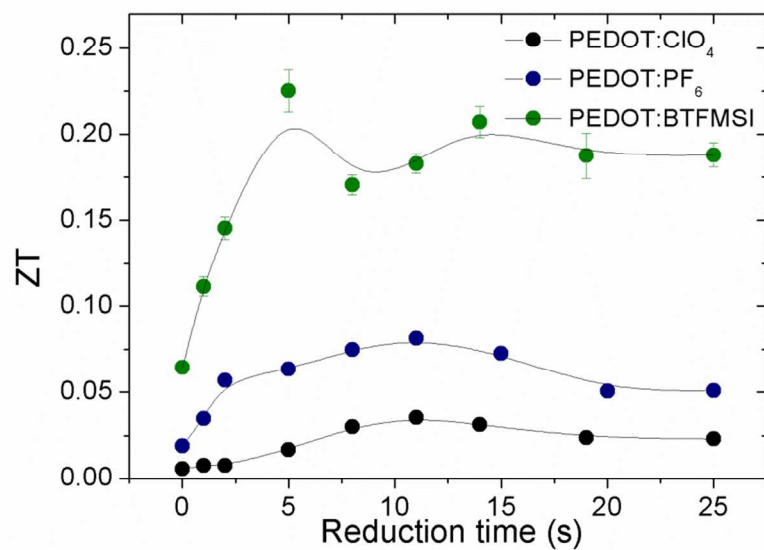**Figure 5**. PEDOT conformation under the presence of different counter-ions

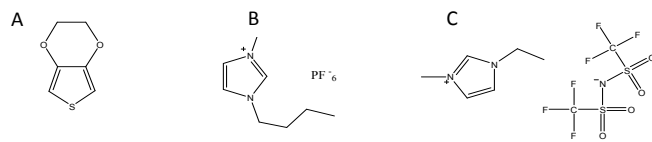**Figure 6**. *ZT* values of PEDOT:ClO$_4$, PEDOT:PF$_6$ and PEDOT:BTFMSI as a function of chemical reduction time at 25 °C.

Figure 7. Molecular structure of A: 3,4-Ethylenedioxythiophene, B: 1-Butyl-3-methylimidazolium hexafluorophosphate and C: 1-Ethyl-3-methylimidazolium bis(trifluoromethylsulfonyl)imide.
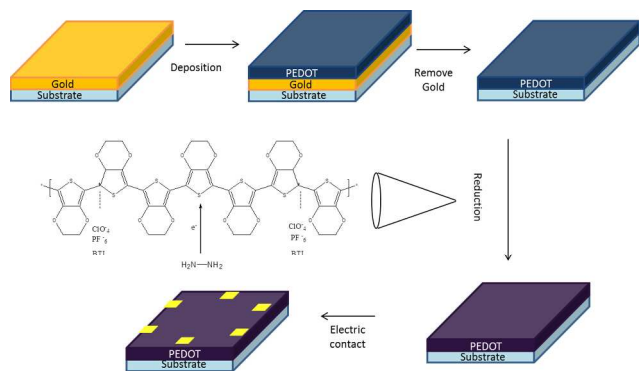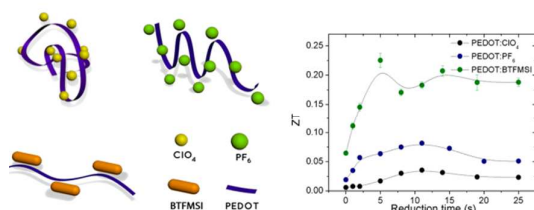

Figure 8. Scheme of the sample preparation sequence.

Enhanced thermoelectric performance of PEDOT with different counter ions optimized by chemical reduction

Mario Culebras, Clara M Gómez and Andrés Cantarero

Thermoelectric properties of different intrinsically conducting polymers based on PEDOT (poly(3,4-ethylenedioxythiophene) doped with several counter-ions: PEDOT:ClO4, PEDOT:PF6 and PEDOT:bis(trifluoromethylsulfonyl)imide have been investigated. The best thermoelectric efficiency has been observed in PEDOT: bis(trifluoromethylsulfonyl)imide, where a ZT value of 0.22, has been deduced from the measurements of the Seebeck coefficient, electrical and thermal conductivity